VOL. 15, NO. 5, MARCH 2020 ISSN 1819-6608
ARPN Journal of Engineering and Applied Sciences

www.arpnjournals.com

OPTIMIZATION OF HIGH-FREQUENCY RESISTANCE WELDING PROCESS USING MECHANICAL PROPERTY OF FINNED TUBE SA-192 STEEL

Montri Sangsuriyun[1], Prayoon Surin[1] and Krittee Eidhed[2]
[1]Department of Advanced Manufacturing Technology, Faculty of Engineering, Pathumwan Institute of Technology, Bangkok, Thailand
[2]Faculty of Engineering, King Mongkut's University of Technology North Bangkok, Bangkok, Thailand
E-Mail: montri.sang@npuac.th

ABSTRACT

The objective of this study is to investigate the effects of welding parameters in the welding process on the mechanical properties and micro structure to compare the design of experiment (DOE) for the high-frequency resistance welding process (HFRW) of ASTM SA-192high-carbon steel. The different butt weld *T* joints of finned-tubes were prepared by varying the welding parameters, including current (A), voltage (kV) and frequency (rpm) which were also related to the heat input and mechanical properties. DOE analysis of the welding parameters was performed at 9A, 13kV, 250 rpm and heat input of 474 J/mm. The results showed that the ultimate tensile strength was 749 MPa which meets the standard requirements of the Association of Finned Tube Manufacturers and is at a good level in the production viewpoint.However, the examination of the micro-and macrostructure of the weld line using an inverted microscope showed some melting on the specimens and it was found that some specimens had high weld width and weld depth. In addition, the tensile strength was also higher. However, too high tensile strength was changed the material structure, the cause of HAZ. Through the validation of the welding process which was compared to the fatigue strength, the following results were indicated: (1) the ultimate tensile strength at the highest tensile stress was not the ultimate fatigue strength and the heat input affected the weld width and weld depth of the weld line. (2) In the welding process, the weld width and weld depth must be also considered since they can affect the specimen failure during the experiment. Therefore, extreme care must be taken when using a high-frequency resistance welding process.

Keywords: welding parameters, mechanical property, resistance welding process, finned-tubes.

1. INTRODUCTION

There are many types of stainless-steel heat exchangers, such as shell and tube heat exchanger, plate heat exchanger and finned tube heat exchanger, etc. The finned tube heat exchanger is widely used and has a variety of applications in industries such as oil refineries, power plants and petrochemical industry due to the advantages of a finned pipe which can improve heat dissipation by increasing heat transfer surface area. Thus, it reduces the number of pipes and related equipment sizes, which can also reduce project costs [1]. The high-frequency resistance welding (HFRW) process is considered as the resistance welding that uses high-frequency current in the welding process. HFRW can generate heat and relies on the compression force in welding the specimen. Besides, controlling the welding speed results in heat conduction during the welding process, which affects the weld depth of the material. If the welding speed decreases, the heat inside the specimen increases, increasing the weld depth of the material [2, 3]. A common problem in the heat exchange of stainless steel is the cracks in the tube and the fin surface. These cracks are caused by stress corrosion cracking (SCC). Local stress level resulting from the combination of loads affects the fracture in the material. Although stainless steel has excellent resistance to fatigue or corrosion, high heat or temperature in the welding process can lead to cracks and risk of corrosion. SCC is induced by stress along with the exposure of the corrosive environment [4, 5, 6]. In addition, fatigue caused by external forces and vibration due to the environment affects the optimization of welding parameters or welding processes, because unsuitable parameters accelerate cracking and corrosion [7, 8].

Therefore, this study aimed at determining the optimum parameters by using the Design of Experiment (DOE) principle for the high-frequency resistance welding process and the comparison the mechanical properties of the material, including tensile stress, fatigue and macro- and microstructure of SA-192 finned tube, the causes of failure in welding of pipe and fin.

2. EXPERIMENTAL PROCEDURE

2.1 Materials and welding standards

In this study, the finned tube heat exchanger was investigated. This heat exchanger was made of ASTM SA-192 high-carbon steel with 0.6-0.18% C, 0.27-0.63% Mn, 0.25% Si, 0.035% P and 0.035% Sand with 0.83mm diameter and 3.2 mm wall thickness. The fin was 16mm high and 1mm thick shown in Figure-1. The tests were conducted in accordance with the finned tube production standard [9].

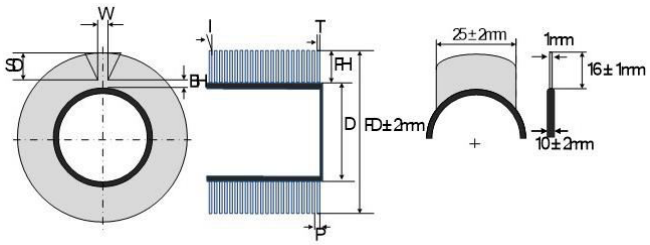

Figure-1. Shape and dimensions of finned tube.

2.2 Experimental design

The study procedures for determining the optimum parameters for the high-frequency resistance welding process with the characterization of mechanical properties of SA-192 finned tube are as follows:

2.2.1. In the HFRW of the finned tube, seven specimens with butt weld joint were prepared (shown in Figure-2), including FT-1, FT-2, FT-3, ..., FT-7by varying the welding parameters which were important factors in the design. The three independent factors were a voltage (kV), current (A) and frequency (rpm) and the dependent factor was heat input (J/mm).

2.2.2 The results of all 7 specimens in Section

2.2.1 were used to create the model using MINITAB 18 software and the Multilevel Factorial Design was used.

2.2.3. Analysis of micro- and macrostructure all 7 specimens

2.2.4. Tensile strength test all 28 specimens

2.2.5. Fatigue test all 28 specimens

2.2.6. Analysis of micro- and macrostructure of all 7 specimens after the fatigue test.

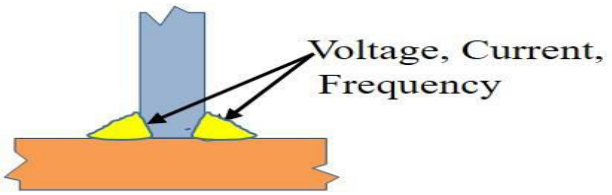

Figure-2. Butt weld joint of finned tube.

2.3 Standards

In this study, the size of the finned pipe was set at ±2mm according to the international standard for dimensions, tolerances, and tests of HFR Was shown in Figure-3.

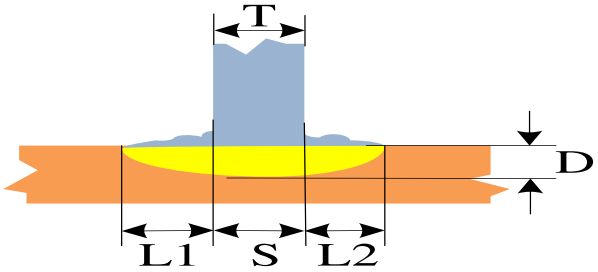

Figure-3. Ratio of weld width and penetration.

T = fin thickness is 1000 µm
D = weld depth (mm)
S = weld width (mm)
L = excess weld metal

2.4 Melting and weld depth determination

The International Standard for Dimensions, Tolerances and Tests of High Frequency Resistance Welding considers the specimen using the acceptance criteria (Q) by measuring S (weld width (mm)) and D (weld depth (mm)) values from the microstructure micrograph in order to prevent the measurement error according to the requirements of the standard [11]. The requirements or the acceptance criteria of weld width are that the weld width must be ≥ 90% of fin thickness which is can be calculated using equation (1) and the weld depth must be in the range of0.05 - 0.30 mm.

a) Weld width: Q = (S/T) x 100
When T = Nominal thickness of fin (mm)
S = Weld Width (mm)
Acceptance Criteria: Q ≥ Average 90% of nominal fin thickness
b) Weld Depth
Acceptance Criteria: 0.05 < D < 0.30 mm

2.5 Tensile strength test

Tensile strength test was performed with all 7 specimens in order to determine the tensile strength of finned-tube. The tensile feed velocity was 0.2 mm/min. The tensile strength test was performed in triplicatepertreatment in which the standard ultimate tensile strength (UTS) must be higher than that of based on the Finned Tube at 500 MPa [12]. The average value was calculated.

2.6 Fatigue test

The Fatigue test was performed with all 7 specimens at a constant load speed of 1 kN/s, the target load was chosen as1.5MPa, 3 MPa, 6 MPa, 9 MPa.The tighten speed of 1 mm/s in sine wave control mode, channel frequency 10, amplitude 3 and at room temperature using Jinan Tengri Test Equipment IE Corporation. 10 kN Load was used [10].

2.7 Micro- and macrostructure test

Micro-and macrostructure examination of all 7 specimens was performed using Zeiss Vert A1inverted microscope. In addition, the initiation and expansion of cracks on the surface were also examined using a scanning electron microscope (SEM).

3. RESULTS

3.1 Effects of the specimen on tensile strength and heat input

Figure-4 shows the comparison of the tensile strength of the specimens at a constant strain rate until the fracture of the specimens. The results showed that the fractures of FT-2 and FT-3 occurred between the fin and tube and did not meet the UTS standard at 500 MPa. This

indicates that low melting and welds depth results in low tensile strength as a result of too low heat input for material melting.

For FT-1, FT-4, FT-5, FT-6 and FT-7, it was found that FT-7 had the highest tensile stress of 749 MPa and heat input of 467 J/mm. This was because the welding condition met the standard UTS value of more than 500 MPa which also resulted in higher highest tensile stress.

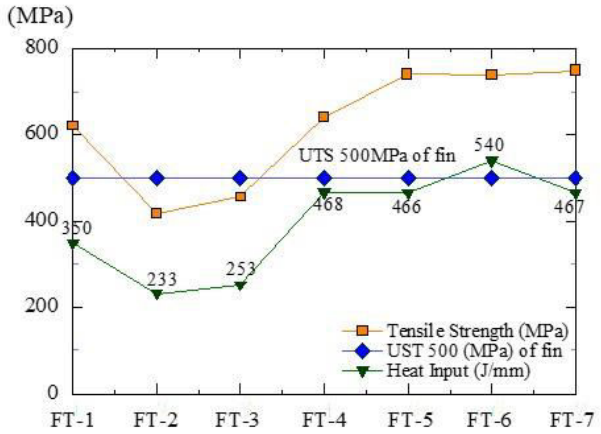

Figure-4. Comparison of tensile strength, UTS 500MPa of the fined tube and heat input of 7 specimens.

3.2 Determination of weld width and weld depth between in and tube

Figure-5 shows the determination of weld width and weld depth between fin and tube for FT-2 and FT-3 which did not meet the standards of the Association of Finned Tube Manufacturers. Considering the weld width and weld depth, the low current (A) and voltage (kV) and high frequency (rpm) resulted in no melting and weld depth which was the causeo flow heat input.

For specimens that met the requirements of the Tensile Strength Test, including FT-1, FT-4, FT-5, FT-6, and FT-7, the fracture must occur only at the fin. As a result, adjustment of the welding parameters such as the heat input. It was found that the heat input affected the weld width and weld depth of the welding line between fin and tube. In the case of the adjustment of the low level of the current (A) and the voltage (kV), while the high level of the frequency (rpm), the magnitude of the heat input was 200≤290 (J/mm). It was caused that of the low annealing in the specimens. In the case of adjusting the height level of the current (A) and the voltage (kV), while the low frequency (rpm). It was shown that the magnitude of the heat input was 350 ≥ 540. It was found that the appropriate condition of the welding parameter was that the current was 13 kV, the voltage was 9 Amp and the frequency was 250 rpm, the heat input was 474 J/mm. The appropriate condition of the weld width and weld depth between the fin and tube was affected to the tensile strength. For FT-1, the examination of the weld line showed that there were some melting and the weld width was 511.037 µm with no melting at L1 weld line while L2 line was 606.394 µm wide. The heat input was 350 J/mm which was lowest compared to the specimens that met the standard requirements. In other words, low heat distribution results in low weld depth, resulting in less change in the material structure. FT-4, FT-5, FT-6, and FT-7 showed complete melting. The current, voltage and frequency values of these specimens were between 9-10 A, 13-15 kV and 250 - 300 rpm, respectively and heat input values were between 466 - 540 J/mm. In other words, the optimum heat distribution results in deep penetration, resulting in a change in the material structure.

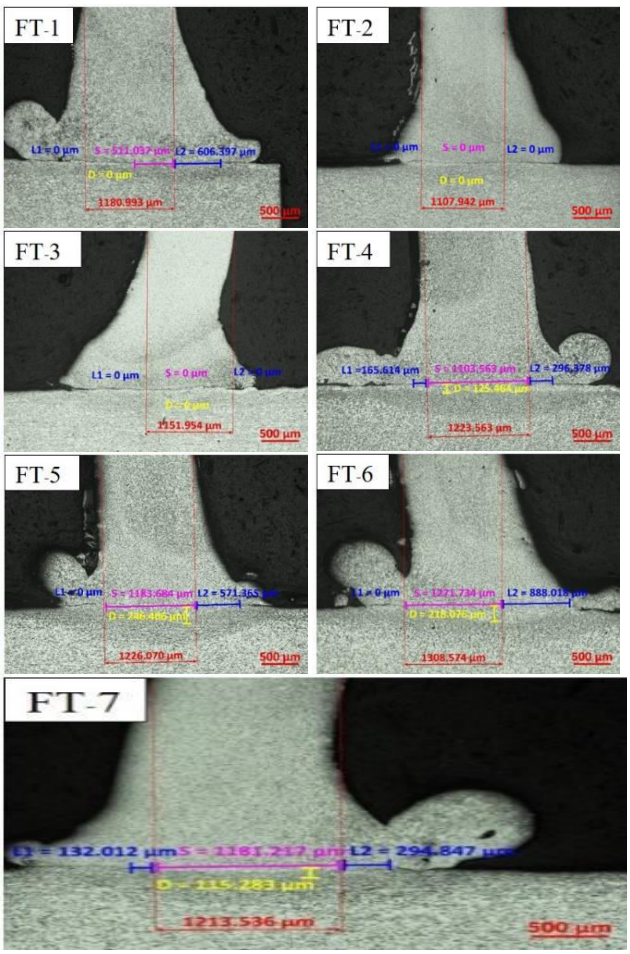

Figure-5. Determination of weld width and weld depth.

3.3 Statistical analysis of factors affecting the welding process

Figure-6 shows the results of the validation and goodness of fit of the model. Normal Probity Plot revealed the normal distribution and the Versus Fits showed the linear trend of errors. In addition, the histogram of error values was bell-shaped. From the determination of Versus Order, the error terms were considered independent.

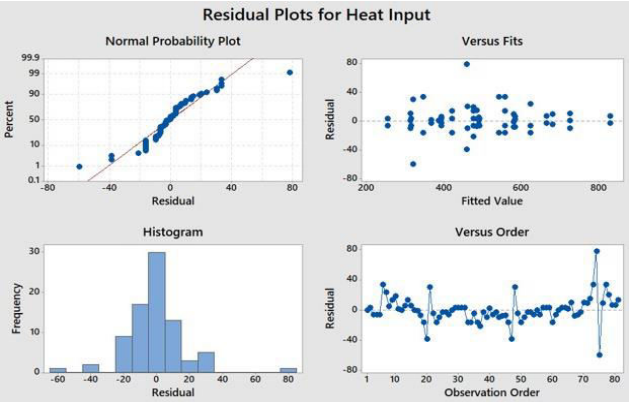

Figure-6. Data characterization.

In Figure-7, it can be observed that the important factors in the multilevel factorial design such as current, voltage and frequency affected the HFRW process. Both main factors A, B and C and the interaction terms AC, AC, and AB had significant effects on heat input at a significant level of 0.05. Figure-8 shows the determination of the optimum parameters for the welding process which it was found that the optimum condition was 9 A, 13 kV, 250 rpm and heat input of 474 J/mm. Figure-9 shows the Main Effects Plot for Heat Input Fitted Mean in the welding process of fin and tube.

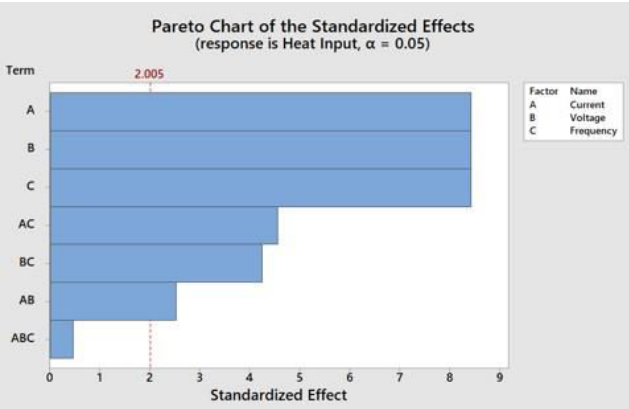

Figure-7. Factors affecting the HFRW process.

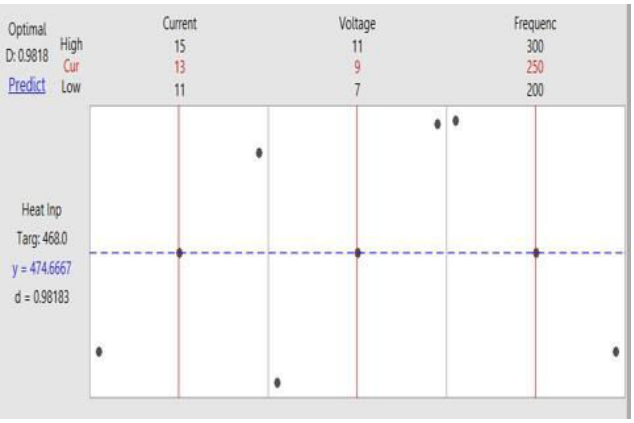

Figure-8. Parameter optimization.

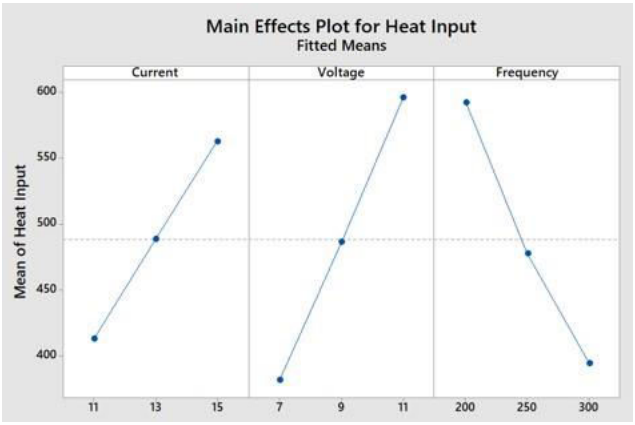

Figure-9. Main Effects Plot for Heat Input Fitted Mean.

3.4 Effects of the specimen on fatigue

All 7 specimens (3 parameters) had different heat input. Figure-10 shows S-N curve of FT-2 and FT-3 finned tubes which did not meet the standard requirements of the Association of Finned Tube Manufacturers. In the fatigue test, the failure was observed immediately at the highest load of 1 kN and $10^7 N_f$, and the weld width and weld dept were small.

The specimens that met the standard requirements of the Association of Finned Tube Manufacturers included FT-1, FT-4, FT-5, FT-6, and FT-7.

For FT-1, the characterization of the welded joint showed some weld pool and fatigue strength of1.1 kN at 10^7 N_f (cycles) which resulted in the inappropriate heat input due to low weld width.

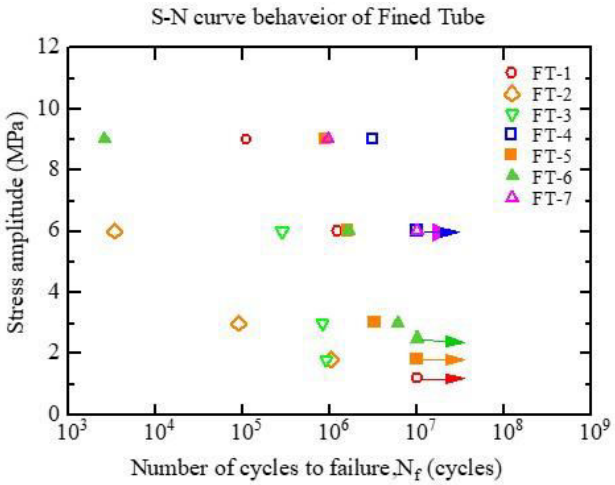

Figure-10. S-N of Finned Tube. The effects of material behavior on fatigue.

For FT-5 and FT-6, the fatigue strength values were 1.8 kN at $10^7 N_f$and 2.5 kN at$10^7 N_f$, respectively. Higher heat input and rotational speed resulted in deeper weld depth between fin and tube, leading to the structural change. The descending order of cooling rate of the material was as follows: (Liq.)>(δ-Ferrite+Liq.)>(δ-Ferrite+γ)>(γ)>(α-Ferrite+γ)>(α-Ferrite+Pearlite). Pearlite and ferrite areas could with stand the highest heat to the

melting point and the fine grain structure had a high hardness which resulted in higher tensile strength in the weld line. However, the fatigue test showed a decrease of strength due to the incomplete weld line at L1. The fatigue during the experiment can cause small cracks on the material surface and these small cracks can progress in to the bigger one (Progressive Crack Growth across the Part).

The highest fatigue strength FT4 and FT-7were similar whichwas6 kN at 10^7N_f. The optimum parameters of the welding process resulted in the optimum weld width and weld depth between L1 and L2 and the complete weld line. The author noted that under the unforeseen operating conditions at 9 kN load, FT-7 could with stand the fatigue cycles of 0.4 x 10^5 N_f. From the optimization plot in Figure-8, it was found that the optimum welding parameters were 13 kV, 9 A, and 250 rpm which resulted in 474 J/mm heat input. However, it was not the optimum value in this study. It can be seen that the most suitable method for the welding parameter optimization is to have an experienced machine operator together with the comprehensive observation in the actual situation. In this study, the fatigue resistance of FT-4 was 3.1 x 10^6N_f, resulting in higher strain intensity in the material.

Figure-11 shows the microstructure of fracture observed under the scanning electron microscope. The SEM micrograph shows fatigue striation, the failure from high stress (a) fatigue fracture surface at 6 kN load and 4.1 x 10^6N_f. The cyclic stress resulted in cracks away from the melt pool of the weld line or heat affected zone (HAZ). At this heat-affected zone, the strength decreased, and the fatigue crack propagated within the specimen. The specimen eventually had a smaller bearing area which led to overload zone and fast fracture. This figure shows the ductile failure with grooves, holes, elongation and eventually fracture. While (b) shows the final fracture surface at 3 kN load and 7.7 x 10^6N_f. The first stepiscrack initial in which small cracks are formed on the material surface. The second stepiscrack propagation, a result of repeated loading at a low frequency which causes low cycle fatigue failure. In this step, the surface of the specimen begins to break into layers, resembling the lines left by the waves on the beach.The last step is a final failure, the sudden failure of the remaining area causing the irreversible damage to the material.

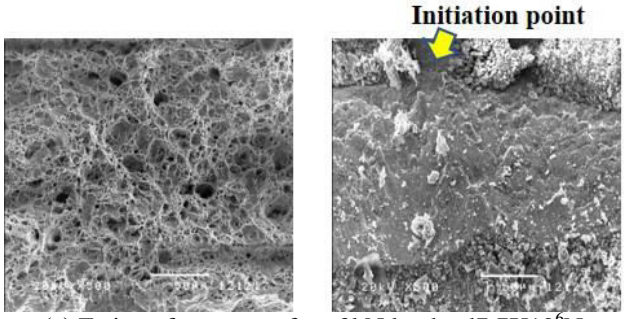

(a) Fatigue fracture surface 3kN loadand7.7X10^6N_f
(b) Final fracture surface at 6 kN load and4.1X10^6N_f

Figure-11. The microstructure of initial surface crack observed under SEM.

4. CONCLUSIONS

- Heat input affected the area, weld width and weld depth between fin and tube.
- Compared to the fatigue strength, the ultimate tensile strength at the highest tensile stress was not the ultimate fatigue strength and heat input affected the weld width and weld depth of the weld line.
- The highest fatigue strength was observed in FT-4at 6 kN load. The failure of FT-7occurred before FT-4 when increasing the load from 6 kN to 9 kN. This was because the heat-affected zone (HAZ), the result of parameter adjustment including heat input and weld width, affected the ultimate fatigue strength, weld depth, and ultimate tensile strength.
- Higher-strength of the weld line in FT-4 and FT-7 affected the tensile strength.
- From the fatigue test and microstructure of the fin of the specimen that met the standard requirements, it was found that the fatigue occurred during using the specimen could cause fatigue failure (fatigue failure testing).
- Using the DOE principle to calculate the optimum parameters for the welding process of fin and tube is an alternative way to determine the optimum condition for various applications.

REFERENCES

[1] JEONG Jin; KIM CHANG NYUNG; YOUN Baek. 2006. A study on the thermal contact conductance in fin-tube heat exchangers with 7 mm tube. International journal of heat and mass transfer. 49.7-8: 1547-1555.

[2] Cynthia L. Jenney, Annette O'Brien. 2007. AWS Welding Handbook. 7th ed. U.S.A. American Welding Society Inc.

[3] Na Y. S., *et al*. 2009. Failure analysis of welded finned tube used in petrochemical plant. Engineering Failure Analysis. 16.6: 1889-1893.

[4] K. I. M. Seonhwa, *et al*. 2018. Failure analysis and structural improvement for cracked circular finned tube. Engineering Failure Analysis. 92: 95-106.

[5] X. U. Shugen; W. A. N. G. Chong; W. A. N. G. Weiqiang. 2015. Failure analysis of stress corrosion cracking in heat exchanger tubes during start-up operation. Engineering Failure Analysis. 51: 1-8.

[6] CHAHARDEHI ABFSA; BRENNAN Feargal P.; STEUWER Axel. 2010. The effect of residual stresses arising from laser shock peening on fatigue crack growth. Engineering Fracture Mechanics. 77.11: 2033-2039.

[7] ASYIKIN, Muhammad Tedy. CFD simulation of vortex induced vibration of a cylindrical structure. 2012. Master's Thesis. Institutt for bygg, anleggog transport.

[8] Warinsiriruk E., Greebmalai J. & Sangsuriyun M. 2019. Effect of Double Pulse MIG Welding on Porosity Formation on Aluminium 5083 Fillet Joint. In MATEC Web of Conferences (Vol. 269, p. 01002). EDP Sciences.

[9] https://tulsafintube.com/wp-content/uploads/2015/03/International-Standard-for-High-Frequency-Welded-Fins-Download.pdf.

[10] Dale James L. 2004. Stud welded pin fin heat sink. U.S. Patent No. 6, 807, 059. 19 Oct.

[11] Boiler A. S. M. E. and Pressure Vessel Code. 2007. Welding and Brazing Qualifications. ASME Section IX.

[12] Bringas J. E. 2004. Handbook of comparative world steel standards. ASTM International.